Evidence for a Role of the Lumenal M3-M4 Loop in Skeletal Muscle Ca^{2+} Release Channel (Ryanodine Receptor) Activity and Conductance

Ling Gao, David Balshaw, Le Xu, Ashutosh Tripathy, Chunlin Xin, and Gerhard Meissner
Departments of Biochemistry and Biophysics, and Molecular and Cellular Physiology, University of North Carolina, Chapel Hill, North Carolina 27599-7260 USA

ABSTRACT We tested the hypothesis that part of the lumenal amino acid segment between the two most C-terminal membrane segments of the skeletal muscle ryanodine receptor (RyR1) is important for channel activity and conductance. Eleven mutants were generated and expressed in HEK293 cells focusing on amino acid residue I4897 homologous to the selectivity filter of K^+ channels and six other residues in the M3-M4 lumenal loop. Mutations of amino acids not absolutely conserved in RyRs and IP_3Rs (D4903A and D4907A) showed cellular Ca^{2+} release in response to caffeine, Ca^{2+}-dependent [^{3}H]ryanodine binding, and single-channel K^+ and Ca^{2+} conductances not significantly different from wild-type RyR1. Mutants with an I4897 to A, L, or V or D4917 to A substitution showed a decreased single-channel conductance, loss of high-affinity [^{3}H]ryanodine binding and regulation by Ca^{2+}, and an altered caffeine-induced Ca^{2+} release in intact cells. Mutant channels with amino acid residue substitutions that are identical in the RyR and IP_3R families (D4899A, D4899R, and R4913E) exhibited a decreased K^+ conductance and showed a loss of high-affinity [^{3}H]ryanodine binding and loss of single-channel pharmacology but maintained their response to caffeine in a cellular assay. Two mutations (G4894A and D4899N) were able to maintain pharmacological regulation both in intact cells and in vitro but had lower single-channel K^+ and Ca^{2+} conductances than the wild-type channel. The results support the hypothesis that amino acid residues in the lumenal loop region between the two most C-terminal membrane segments constitute a part of the ion-conducting pore of RyR1.

INTRODUCTION

Ryanodine receptors (RyRs) control diverse cellular functions by releasing Ca^{2+} from intracellular stores in the sarco/endoplasmic reticulum. RyRs are composed of four 560-kDa RyR subunits and four 12-kDa FK506 binding proteins (FKBPs) (Coronado et al., 1994; Meissner, 1994; Sutko and Airey, 1996; Franzini-Armstrong and Protasi, 1997). They are cation-selective channels that have an unusually high conductance for both mono- and divalent cations and are regulated by various endogenous and exogenous effectors. Cryoelectron microscopy and 3-D image analysis reveal a large, loosely packed 29 × 29 × 12 nm cytosolic foot region and a smaller transmembrane domain (Serysheva et al., 1995; Wagenknecht et al., 1996).

Each of the large RyR polypeptides comprises ~5000 amino acids with four (Takeshima et al., 1989) to as many as 12 (Zorzato et al., 1990) membrane-spanning segments in the C-terminal region, which have been predicted to form the Ca^{2+} channel pore region of skeletal muscle RyR (RyR1). The four membrane-spanning segment model is supported by single-channel recordings with tryptic fragments (Callaway et al., 1994) and deletion mutants (Bhat et al., 1997a,b). The remaining amino acids of RyRs form the large catalytic cytoplasmic foot structure. Studies using site-directed antibodies suggest that the N- and C-termini of RyR1 are cytoplasmically localized (Marty et al., 1994; Grunwald and Meissner, 1995) and show evidence that two sarcoplasmic reticulum (SR) lumenal segments are localized between putative transmembrane segments M1 and M2 and between M3 and M4 (Grunwald and Meissner, 1995), as proposed by Takeshima et al. (1989).

The lumenal loop region between the two most C-terminal membrane segments of RyRs (M3 and M4) has sequence similarities to segments of the related inositol 1,4,5-trisphosphate receptors (IP_3Rs) and at least two otherwise unrelated classes of ion channels, the voltage-gated cation channels and the ligand-gated glutamate receptors (Grunwald, 1996). Recent x-ray analysis confirmed that the region between the two membrane-spanning segments of a K^+ channel from *Streptomyces lividans* extends into the membrane to form part of the ion conductance pathway (Doyle et al., 1998). An important finding was that a conserved VGYG motif comprised the ion selectivity filter of the K^+ channel. A sequence that is related to the K^+ channel VGYG motif is a highly conserved GGIG motif in the M3-M4 lumenal loop of RyRs (Fig. 1).

In this study we tested the hypothesis that the lumenal loop between M3 and M4 of RyR1 plays an important role in channel function. We generated 11 single-site mutants, focusing on one amino acid residue shown to be part of the selectivity filter of K^+ channels (Tyr in K^+ channel, Ile^{4897} in RyRs, and Ile or Val in IP_3Rs), and a second residue (Asp^{4899}) that is highly conserved among the RyR and IP_3R families. The results suggest that the M3-M4 loop is important in determining channel function, particularly with re-

Received for publication 8 September 1999 and in final form 21 April 2000.
Address reprint requests to Dr. Gerhard Meissner, Department of Biochemistry and Biophysics, University of North Carolina, Chapel Hill, NC 27599-7260. Tel.: 919-966-5021; Fax: 919-966-2852; E-mail: meissner@med.unc.edu.

0006-3495/00/08/828/13 $2.00

FIGURE 1 Alignment of putative pore sequences of RyRs. Shown are the putative M3-M4 lumenal loop region of RyRs, the identical residues between RyRs, between the RyR and IP_3R superfamily, and the sequence of the selectivity filter of the K^+ channel from *S. lividans* (Doyle et al., 1998). Also indicated are the residues that were mutated (for properties of mutants see Table 1).

gard to channel conductance, and hence contributes to the ryanodine receptor pore structure. A preliminary report of this work has been presented in abstract form (Gao et al., 1999).

EXPERIMENTAL PROCEDURES

Materials

HEK293 cells were obtained from the Tissue Culture Facility of Lineberger Cancer Center at University of North Carolina. [^{3}H]Ryanodine was obtained from Dupont NEN, unlabeled ryanodine from Calbiochem (La Jolla, CA), and phospholipids from Avanti Polar Lipids (Birmingham, AL). All other chemicals were of analytical grade. Expression vector pCMV5 was generously provided by Dr. David Russel (University of Texas Southwestern Medical Center, Dallas, TX).

Site-directed mutagenesis

The full-length rabbit RyR1 cDNA was constructed as described previously (Gao et al., 1997). Single and multiple base changes were introduced by pfu polymerase-based chain reaction, using mutagenic oligonucleotides and the QuickChange site-directed mutagenesis kit (Stratagene, La Jolla, CA). The C-terminal fragment (*Cla*I/*Xba*I, 14443/15276) of RyR1 cDNA cloned into pBluescript vector served as the template for mutagenesis. Mutated sequences were confirmed by sequencing, and mutated C-terminal fragments were reintroduced into the *Cla*I and *Xba*I sites of the C-terminal fragment of RyR1. Mutated full-length expression plasmids were prepared by ligation of three fragments (*Cla*I/*Xho*I, *Xho*I/*Eco*RI, *Eco*RI/*Xba*I containing the mutated sequence) and expression vector pCMV5 (*Cla*I/*Xba*I) as previously described (Gao et al., 1997).

Expression of wild-type and mutant RyRs

RyR1 cDNAs were transiently expressed in HEK293 cells with the Lipofectamine Plus (Gibco BRL, Grand Island, NY) method, according to the manufacturer's instructions. Cells were maintained in high glucose Dulbecco's minimum essential medium (DMEM-H) containing 10% fetal bovine serum at 37°C and 5% CO_2 and plated the day before transfection. For each 10-cm tissue culture dish, 6 μg DNA was used at a DNA/lipofectamine ratio of 1:3 to 1:5. Cells were harvested 42–48 h after transfection.

Intracellular Ca^{2+} release

Cellular Ca^{2+} release in response to caffeine was measured by intracellular Rhod-2 fluorescence, using a BioRad MRC-600 confocal microscope. Transfected cells were grown on no. 1.5 glass coverslips coated with rattail collagen and loaded with 5 μM Rhod-2 AM in Hanks' balanced salt solution (HBSS) with 2 mM Ca^{2+} and 1.5 mM Mg^{2+} for 30 min at 37°C after thorough washing in that same buffer. The loaded cells were washed three times with Ca^{2+}/Mg^{2+}-supplemented HBSS. Images were recorded before and after the addition of 10 mM caffeine to the Ca^{2+}/Mg^{2+} HBSS bath. These images were then translated into pseudocolor with Photoshop v 5.02 (Adobe, San Jose, CA). In addition to visual analysis of caffeine-induced Ca^{2+} release, the confocal images were quantitatively analyzed with ScionImage (Scion Corp., Frederick, MD). Mean pixel values after background subtraction for each cell in a given coverslip were determined for images recorded before and after the addition of caffeine. The ratio of the mean pixel values before and after the addition of caffeine was then determined (mean after/mean before) and plotted in a histogram including all coverslips obtained for each sample.

Preparation of membrane fractions

Cells were washed twice with 4 ml ice-cold phosphate-buffered saline containing 1 mM EDTA and protease inhibitors (0.2 mM Pefabloc, 100 nM aprotinin, 50 μM leupeptin, 1 μM pepstatin, and 1 mM benzamidine) and harvested in the same solution by removal from the plates by scraping. Cells were collected by centrifugation and stored at −80°C. To prepare membrane fractions, cell pellets were resuspended in the above solution and homogenized with a Tekmar Tissumizer for 5 s at a setting of 13,500 rpm. Cell homogenates were centrifuged for 1 h at 35,000 rpm in a Beckman Ti50 rotor. Membranes were resuspended in a buffer containing 10 mM imidazole (pH 7.0), 0.1 M KCl, 0.3 M sucrose, 20 μM leupeptin, and 0.2 mM Pefabloc.

[^{3}H]Ryanodine binding

Unless otherwise indicated, membranes of 1/12 culture dish were incubated with 2 nM [^{3}H]ryanodine at room temperature in 100 μl of a buffer containing 20 mM imidazole (pH 7.0), 0.25 M KCl, 0.15 M sucrose, 0.2 mM Pefabloc, 10 μM leupeptin, and the indicated free Ca^{2+} concentrations. Nonspecific binding was determined using a 1000-fold excess of unlabeled ryanodine. After 20 h, aliquots of the samples were diluted with 20 volumes of ice-cold water and placed on Whatman GF/B filters preincubated with 2% polyethyleneimine in water. Filters were washed with 3 $\times$ 5 ml ice-cold 0.1 M KCl, 1 mM potassium piperazine-*N,N′*-bis(2-ethanesulfonic acid (KPIPES) (pH 7.0). The radioactivity remaining with the filters was determined by liquid scintillation counting to obtain bound [^{3}H]ryanodine.

Isolation and reconstitution of expressed RyRs

RyRs from two to four culture dishes were solubilized for 10 min at room temperature in 1.5 ml of a buffer containing 5 mg/ml phosphatidylcholine and 1.45% 3-[(3-cholamidopropyl)dimethylammonio]-1-propane-sulfonate (CHAPS) and isolated as 30S RyR complexes by rate density centrifugation (Gao et al., 1997). To detect the 30S RyR complexes on the gradients, solubilized rabbit skeletal muscle SR vesicles were labeled with 2 nM [^{3}H]ryanodine and centrifuged on a parallel gradient. For single-channel measurements, pooled RyR gradient peak fractions were reconstituted into proteoliposomes by removal of CHAPS by dialysis (Lee et al., 1994).

Single-channel recordings

Single-channel measurements were made by incorporating expressed RyR channels in Mueller-Rudin-type lipid bilayers (Tripathy et al., 1995). Unless otherwise indicated, proteoliposomes containing the expressed RyRs were added to the *cis* chamber of a bilayer apparatus and fused in the presence of an osmotic gradient (250 mM *cis* KCl/20 mM *trans* KCl in 20 mM KHEPES, pH 7.4) with planar lipid bilayers containing a 5:3:2 mixture of bovine brain phosphatidylethanolamine, phosphatidylserine, and phosphatidylcholine (50 mg of total phospholipid/ml of *n*-decane). After the appearance of channel activity, further fusion of proteoliposomes was prevented by increasing *trans* KCl to 250 mM. The *trans* side of the bilayer was defined as the ground. Unless indicated otherwise, additions were made to the *cis* bilayer chamber because the large cytosolic regulatory region of native channels faced the *cis* (cytosolic) chamber in a majority (>98%) of the recordings (Tripathy et al., 1995). Unless otherwise indicated, electrical signals were filtered at 2 kHz, digitized at 10 kHz, and analyzed as described (Tripathy et al., 1995). Single-channel recordings of Ca^{2+} current acquired in symmetrical 250 mM KCl with 4 μM *cis* and 10 mM *trans* Ca^{2+} were filtered at 300 Hz.

RESULTS

In the present study, we mutated 11 amino acids in RyR1 to test the hypothesis that the SR lumenal loop linking transmembrane segments M3 and M4 (Fig. 1) is important for channel activity and conductance. One amino acid residue previously shown to be part of the selectivity filter of K^+ channels (Tyr in K^+ channel, Ile^{4897} in RyR1; Fig. 1) was mutated to three different amino acids, maintaining the hydrophobic nature of this position but altering the size of the side chain. A second residue (Asp^{4899}) highly conserved among the RyR and IP_3R families and found in many voltage-regulated K^+ channels was also mutated to three different amino acids, altering the charge at this position. Also mutated were other charged residues that are conserved among the calcium release channel superfamily, R4913 and D4917. Other negatively charged residues were mutated that are not completely conserved (D4903) or are conserved only among the ryanodine receptor family and not among the IP_3 receptor family (D4907).

Cellular fluorescence microscopy was used to measure Ca^{2+} release in response to caffeine in transfected human kidney embryo (HEK293) cells. [^{3}H]Ryanodine binding and single-channel measurements were used as in vitro determinations of mutant channel function, pharmacology, and conductance.

After the original submission of this manuscript, Zhao et al. (1999) published the results of several additional mutations in the lumenal loop region linking transmembrane segments M3 and M4 of the cardiac ryanodine receptor (RyR2). The most significant mutation they reported was that of G4824A (RyR2 numbering, analogous to G4894 in RyR1 numbering), which maintains pharmacological regulation but has a greatly reduced single-channel conductance. We mutated this site in RyR1 after the publication of their work and have included results obtained with RyR1 mutant G4894A in the revised manuscript. Another overlapping mutation between the two studies, D4899A, gives comparable results.

Intracellular Ca^{2+} release of RyR1 mutants

The presence of a caffeine-sensitive Ca^{2+} release mechanism in intact transfected HEK293 cells was assessed by monitoring the fluorescence change in Rhod-2 in response to the addition of 10 mM caffeine. Caffeine in the millimolar concentration range is known to activate RyR1 (Rousseau et al., 1988) and has little or no effect on the basal fluorescence of Ca^{2+}-sensitive fluorophores in nontransfected HEK293 cells (Du and MacLennan, 1998). Fig. 2 shows confocal images of Rhod-2 fluorescence in HEK293 cells transfected with cDNA encoding wild-type and mutant RyR1 proteins before (*left panels*) and 30 s after (*right panels*) the addition of 10 mM caffeine. Shown are representative images demonstrating the lack of caffeine-induced Ca^{2+} release in nontransfected HEK293 cells (Fig. 2 *A*) and typical caffeine-induced Ca^{2+} release in wt-RyR1-transfected cells (Fig. 2 *B*). Arrows indicate cells showing an obvious increase in pseudocolor value and hence in cytosolic calcium. Mutations G4894A, D4899A (representative image shown in Fig. 2 *C*), D4899R, D4899N, D4903A, D4907A, and R4913E yielded a caffeine-induced Ca^{2+} release similar to that of wt-RyR1. Mutation D4917A (Fig. 2 *D*) was completely lacking in caffeine-induced Ca^{2+} release in these experiments. The time course of caffeine-induced Ca^{2+} release for I4897L was delayed relative to that observed for wt-RyR1, with Ca^{2+} release becoming

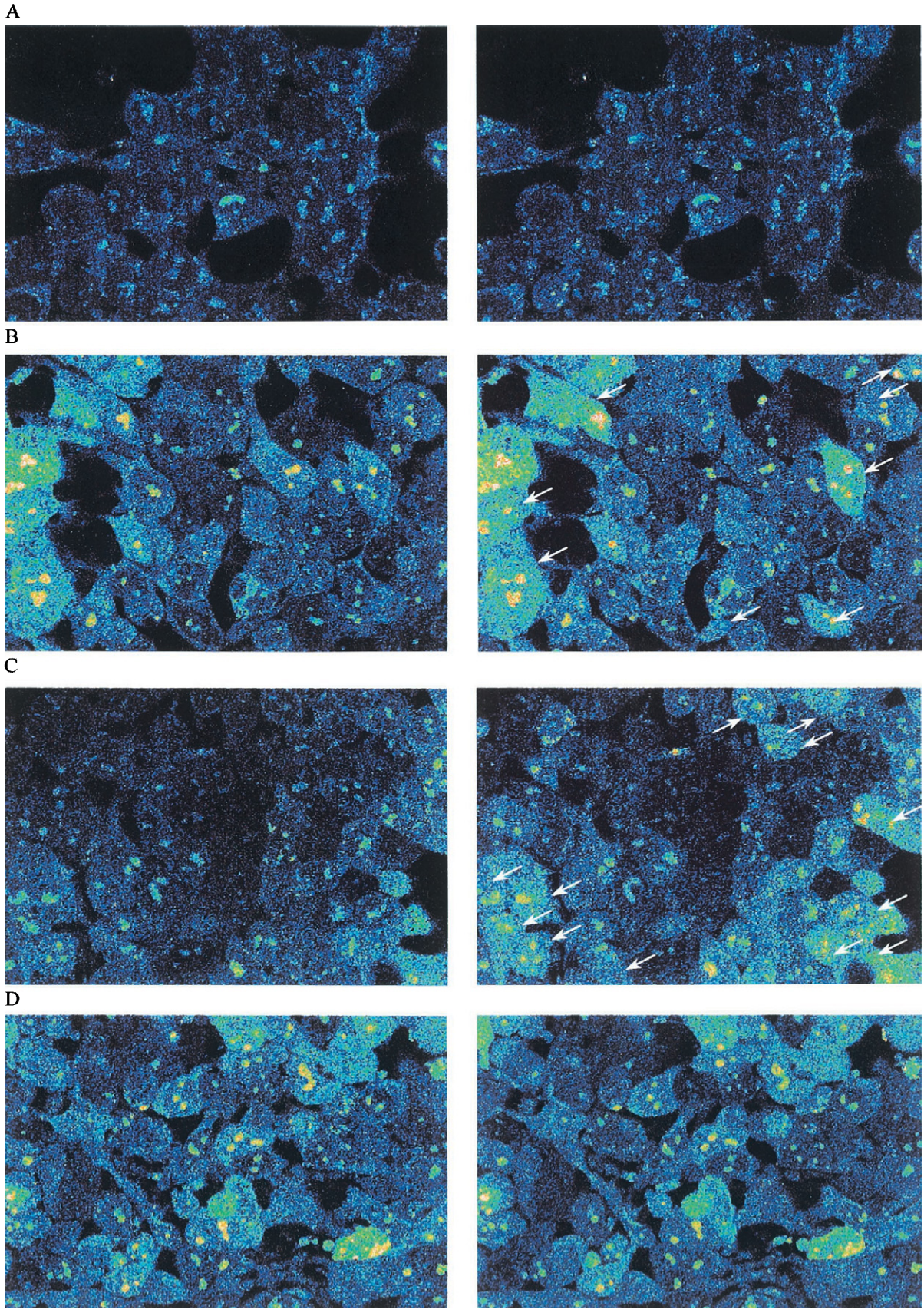
A
B
C
D

apparent 30 s after caffeine addition to the bath, as opposed to the near-immediate Ca^{2+} release observed in wt-RyR1-transfected cells. Mutations I4897A and I4897V had caffeine-induced Ca^{2+} release in a small number of cells that was of very short duration, averaging ~20 s from onset of release to restoration of basal Ca^{2+} levels. These phenomena are not observed in nontransfected or wt-RyR1-transfected cells. The spots of high fluorescence intensity in the confocal images represent Rhod-2 intercalation into chromatin (J. Lemasters, personal communication).

A slightly more quantitative analysis of caffeine response compared the mean pixel value before and after caffeine treatment for individual cells. Control cells, transfected with the vector lacking an insert, showed a slight increase in mean pixel value after caffeine addition with a mean ratio of pixel value of 1.03 ± 0.30 (SD) and were distributed in a roughly Gaussian manner (Fig. 3 *A*). A very low frequency of individual cells (eight of 276 total) had a ratio greater than 1.63; therefore, in further analyzing the mutations, this value was used as a "cutoff" for defining a response to caffeine. Transfection of plasmid DNA encoding the wild-type RyR1 (Fig. 3 *B*) and mutations G4894A, D4899A, N or R, D4904A, D4907A, and R4913E in images acquired 30 s after caffeine addition to the bath, as well as I4897L in images 45 s after caffeine addition resulted in the appearance of several individual cells with ratios greater than 1.63 (summarized in Table 1). That this population is not distributed in a strictly Gaussian manner is not alarming, as there may be cell-to-cell variations in the level of receptor expression in the transfected cells, and the increase in fluorescence will be related to the proportion of the cell within the confocal plane. Transfection with cDNA encoding I4897A or I4897V resulted in the rapid transient appearance of a small population of cells with ratios greater than 1.63 (two of 226 cells for I4897A and one of 168 cells for I4897V). Transfection with cDNA encoding the mutation D4917A (Fig. 3 *C*) failed to result in the appearance of any individual cells with ratios greater than 1.63 (0 of 142 cells). The results from coverslips with caffeine-induced Ca^{2+} release indicate that ~15–50% of the cells were transfected.

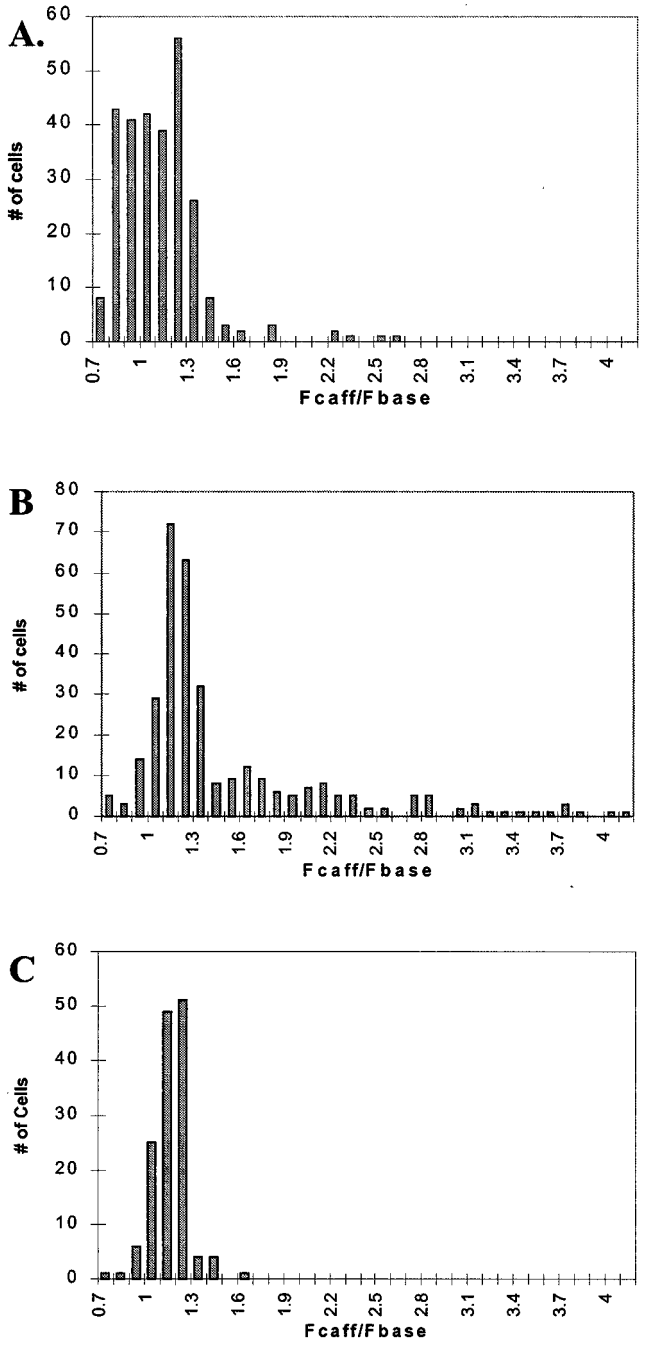

FIGURE 3 Semiquantitative analysis of caffeine-induced Ca^{2+} release in HEK-293 cells. Mean pixel values were determined for each cell in all coverslips used for each mutant receptor before and after the addition of caffeine to the bath. The data are expressed as the ratio of fluorescence with caffeine to fluorescence without. (*A*) Vector-transfected cells. (*B*) wt-RyR1-transfected cells. (*C*) D4917A-transfected cells.

[^{3}H]Ryanodine binding to RyR1 mutants

The expression of functional RyR1 mutant proteins was also assessed by determining their [^{3}H]ryanodine-binding properties. The highly specific plant alkaloid is widely used as a probe of channel activity because of its preferential binding to open RyR ion channel states (Coronado et al., 1994; Meissner, 1994; Sutko and Airey, 1996). Membrane frac-

FIGURE 2 Caffeine-induced Ca^{2+} release in HEK293 cells transfected with wild-type and mutant RyR cDNAs. Confocal images were acquired before (*left column*) and after (*right column*) the addition of 10 mM caffeine to the bath. (*A*) Lack of caffeine response in nontransfected cells. (*B*) Individual cells transfected with wt-RyR1 respond to caffeine (*arrows*), indicating cells with caffeine-induced Ca^{2+} release. (*C*) Representative image of D4899A, showing a typical response for a mutant channel that responds to caffeine stimulus. (*D*) An image acquired for D4917A, indicating a lack of response for those mutants failing to show caffeine-induced Ca^{2+} release.

TABLE 1 Properties of RyR1s mutated in putative pore region

Name	Caffeine-induced Ca^{2+} release in cells (% of cells ratio > 2 × SD)	[^{3}H]Ryanodine binding to cell membranes		Maximum K^+ conductance of purified RyRs (pS)	Ca^{2+} current 10 mM *trans* Ca 0 mV (pA)
		K_d (nM)	Ca^{2+} dependence		
Vector ctrl	2.9	−	−	−	−
wt-RyR1	22.7	12.5 ± 3.5 (5)	+	785 ± 6 (14)	−2.7 ± 0.3 (5)
G4894A	11.1	6.4 ± 2.4 (3)*	as wt-RyR1	21 ± 1 (4)*	~0 (4)*
I4897A	0.9	−	−	322 ± 44 (7)*	−0.2 ± 0.1 (5)*
I4897L	7.3	−	−	436 ± 50 (5)*	−0.5 ± 0.1 (3)*
I4897V	0.6	−	−	432 ± 24 (6)*	−0.2 ± 0.1 (3)*
D4899A	25.7	−	−	626 ± 20 (7)*	−0.5 ± 0.1 (3)*
D4899R	14.2	−	−	390 ± 44 (10)*	−0.1 ± 0.1 (3)*
D4899N	19.3	6.9 ± 1.3 (3)*	as wt-RyR1	87 ± 2 (7)*	−0.4 ± 0.1 (4)*
D4903A	24.6	9.5 ± 1.2 (3)	as wt-RyR1	796 ± 10 (8)	−2.4 ± 0.1 (4)
D4907A	50.0	11.4 ± 1.0 (3)	as wt-RyR1	790 ± 10 (8)	−2.4 ± 0.2 (4)
R4913E	13.6	−	−	297 ± 50 (12)*	−0.4 ± 0.1 (7)*
D4917A	0	−	−	488 ± 63 (12)*	−0.1 ± 0.1 (4)*

−, not detected.
*$P < 0.05$ when compared to wt-RyR1 by unpaired Student's *t*-test.

tions of HEK293 cells transfected with wt-RyR1 cDNA showed a biphasic Ca^{2+} dependence of [^{3}H]ryanodine binding typical of native receptors (Fig. 4). Mutants with an I4897 to A, L, or V substitution all failed to bind [^{3}H]ryanodine. Among the remaining eight mutants, mutations of amino acids not fully conserved (D4903A) among ryanodine and IP_3 receptors or identical only among RyRs (D4907A) showed Ca^{2+}-dependent [^{3}H]ryanodine binding essentially identical to that of wt-RyR1. Scatchard analysis showed an affinity of [^{3}H]ryanodine binding indistinguishable from that of expressed wt-RyR1 (Table 1). Among single-site mutations of amino acid residues highly conserved among the RyR and IP_3R families, only G4894A and D4899N showed detectable [^{3}H]ryanodine binding (Fig. 4) with an approximately twofold increase in [^{3}H]ryanodine binding affinity relative to that observed for wt-RyR1 (Table 1), while D4899A, D4899R, R4913E, and D4917A resulted in loss of detectable high-affinity [^{3}H]ryanodine binding. Absence of [^{3}H]ryanodine binding was not due to lack of expression of the mutant proteins, as immunoblots indicated similar expression levels for all constructs (Fig. 5). Cells transfected with the expression vector alone did not show specific [^{3}H]ryanodine binding.

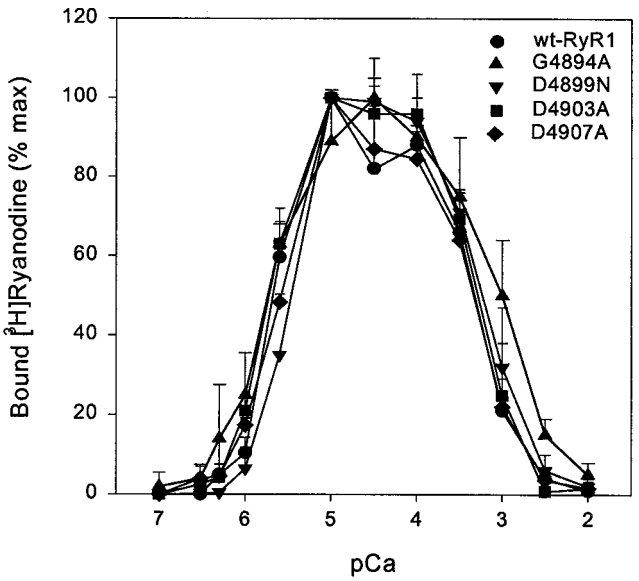

FIGURE 4 Ca^{2+} dependence of [^{3}H]ryanodine binding to wild-type and mutant RyR1s. Specific [^{3}H]ryanodine binding to membranes from cells transfected with wt-RyR1 (●) and mutations of G4894A (▲), D4899N (▼), D4903A (■), and D4907A (♦) was determined in 250 mM KCl, 20 mM imidazole (pH 7.0) media containing 2 nM [^{3}H]ryanodine and the indicated concentrations of free Ca^{2+}. Cells transfected with the expression vector alone or with the other mutant RyRs did not show specific [^{3}H]ryanodine binding. Data are the mean ± SD of three to five experiments.

Single-channel recordings

The presence of an ion conducting activity in the mutant RyR1s was determined in single-channel measurements

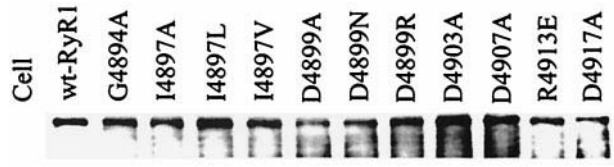

FIGURE 5 Western Blot analysis of protein expression. Transfected cells grown on a 10-cm plate were harvested in 5 ml phosphate-buffered saline. Ten microliters of this sample was loaded into a single lane of a 5% acrylamide gel. After overnight transfer to polyvinyl pyrrolidine fluoride (PVDF), the membrane was blocked in 5% milk with 0.1% Tween-20 and exposed to a monoclonal antibody raised against RyR1 (mAb RyRD110). The secondary antibody was horseradish peroxidase-conjugated anti-mouse.

with the planar lipid bilayer method. In these studies we took advantage of the fact that RyRs are Ca^{2+}-gated channels that are impermeant to Cl^- and conduct monovalent cations more efficiently than Ca^{2+} (Coronado et al., 1994; Meissner, 1994; Sutko and Airey, 1996). The use of K^+ instead of Ca^{2+} as the current carrier therefore afforded a higher resolution of single-channel events.

Fig. 6 shows representative current traces of single wild-type and mutant RyR1 ion channels with K^+ as the current carrier. Proteoliposomes containing the purified 30S channel complexes were fused with planar lipid bilayers, and single channels were recorded in symmetrical 250 mM KCl that contained micromolar activating *cis* (cytosolic) Ca^{2+} concentrations. In the upper trace of Fig. 6, a single partially activated wt-RyR1 was recorded in the presence of 20 μM free cytosolic Ca^{2+} at a holding potential of -40 mV. In symmetrical 250 mM KCl, wt-RyR1 channels had a mean conductance of 785 $\pm$ 6 pS ($\pm$ SE, $n = 14$), which was essentially identical to that of native skeletal muscle RyR1 (Tripathy et al., 1995). Reduction of cytosolic Ca^{2+} to $\sim$70 nM and the increase to 10 mM by adding EGTA and Ca^{2+}, respectively, to the *cis* chamber decreased channel activities to near zero. Thus the purified wt-RyR1 exhibited a K^+ conductance and Ca^{2+} dependence indistinguishable from that of native receptors (Tripathy et al., 1995).

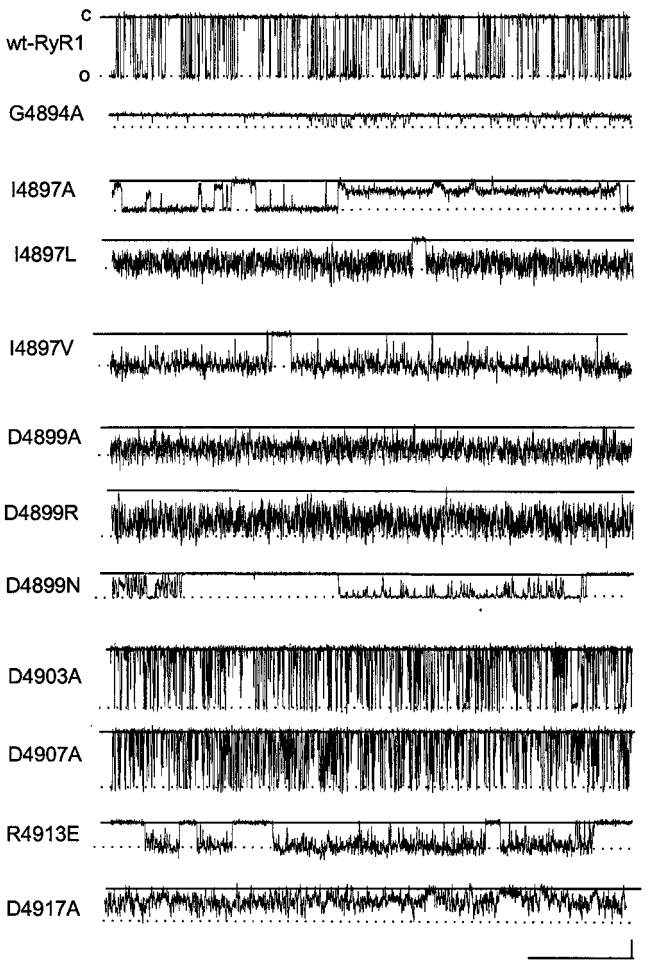

FIGURE 6 Single-channel recordings of wild-type and mutant RyR1s in symmetrical 250 mM KCl solution. Single-channel currents, shown as downward deflections from closed levels (*c, solid line*) to a maximum conductance level (*o, stippled line*), were recorded in 250 mM KCl, 10 mM KHEPES (pH 7.4) media containing 4–20 μM free Ca^{2+}. Traces were acquired at -40 mV and filtered at 2 kHz, with the exceptions of G4894A and D4899N, which were acquired at -70 mV and filtered at 300 Hz. The scale bars are 100 ms and 10 pA for all channels except G4894A and D4899N, which are 200 ms and 2.5 pA and 200 ms and 5 pA, respectively. Maximum K^+ conductance values are given in Table 1.

Channels with I4897 mutated to A, L, or V exhibited an altered K^+ conductance and displayed several intermediate conductance states (Fig. 6, *traces 3–5*, and Table 1). The two mutants with an amino acid substitution not absolutely conserved in RyRs and IP_3Rs (D4903A) or only identical among RyRs (D4907A) had a K^+ conductance and displayed a gating behavior essentially identical to that of wt-RyR1 (Fig. 6, *traces 9* and *10*, and Table 1). Mutation of the conserved G4894 to A (Fig. 6, *trace 2*) and D4899 to N (Fig. 6, *trace 8*) resulted in greatly reduced single-channel conductances (Table 1). The two channels did show several incompletely resolved openings due to filtering at 300 Hz; these do not represent subconductance states. The remaining mutants exhibited an altered K^+ conductance and gating behavior markedly different from those of wt-RyR1 (Fig. 6, *traces 6–7* and *11–12*). These mutants showed segments in which the channel fluctuated between subconductance states and failed to close completely for long periods. Mutations of I4897 (A, L, and V), D4899 (A and R), R4913E (shown in Fig. 7 *A*), and D4917A were open in the presence of mM EGTA in the *cis* chamber (nM *cis* Ca^{2+}), and single-channel open channel probabilities (P_o's) were not significantly affected by changes in *cis* Ca^{2+} for these mutations. Likewise, none of these mutations were modified by *cis* ryanodine at concentrations up to 100 μM.

Figs. 8–10 show three of the four mutations that retain pharmacological regulation: the unconserved D4903A and the highly conserved G4894A and D4899N, respectively. The results for D4903A are identical to those of D4907A as well as wt-RyR1, and therefore these are not shown. Panel *A* in Figs. 8–10 indicates that all three channels show regulation by *cis* Ca^{2+} in a manner similar to that of native RyR1 and to that seen in [^{3}H]ryanodine binding (Fig. 4), with very low P_o in nM *cis* Ca^{2+}, increasing to a peak at $\sim$100 μM *cis* Ca^{2+} before decreasing back to low P_o in mM Ca^{2+}. However, the absolute P_o values varied greatly with maximum P_o (at 100 μM Ca^{2+}), ranging between 0.10 and 0.94 for these mutants with $P_{o,\,max} = 0.38 \pm 0.23$ ($n = 3$) for G4894A, $P_{o,\,max} = 0.52 \pm 0.1$ ($n = 6$) for D4899N, and $P_{o,\,max} = 0.26$ ($n = 2$) for D4903A. By comparison, at 4 μM cytosolic Ca^{2+}, P_o values for G4894A (0.19 $\pm$ 0.07, $n = 5$), D4899N (0.22, $n = 2$), and D4903A (0.10 $\pm$ 0.03, $n = 10$) are lower than the $P_{o,\,max}$ at 100 μM Ca^{2+}. Panel

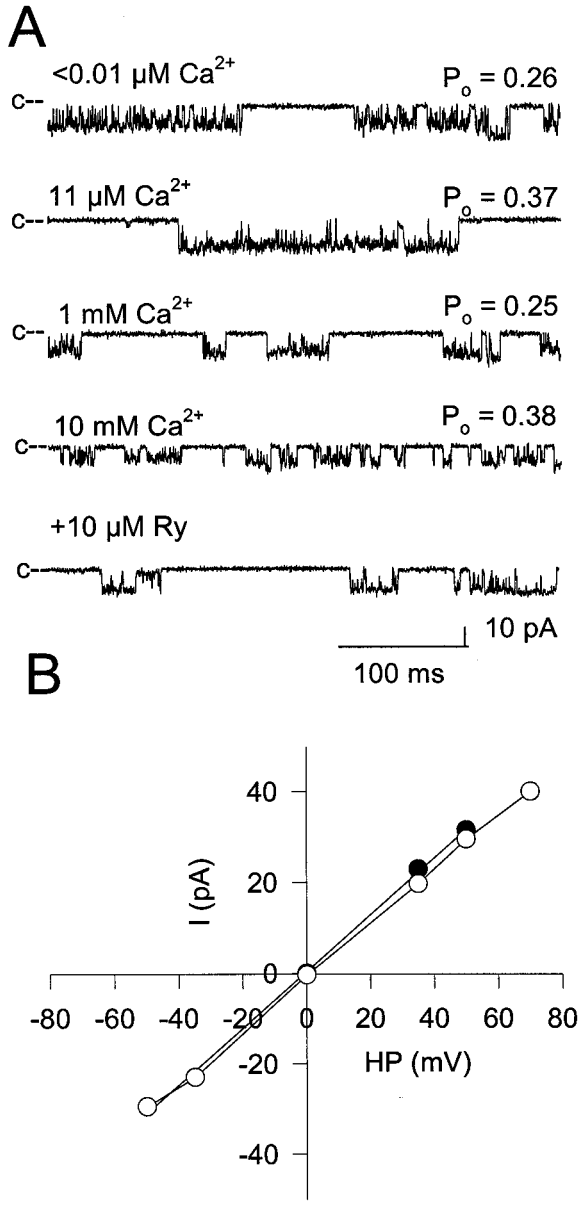

FIGURE 7 Single-channel recordings for mutant R4913E. Single-channel currents were recorded at −35 mV in symmetrical 250 mM KCl and are shown as downward inflections from a closed state (*c*–). (*A*) Effect of varied Ca^{2+} in the *cis* (cytosolic) chamber and the addition of 10 μM ryanodine. (*B*) Current-voltage relationship of the expressed channel in 250 mM symmetrical KCl (●) and with the subsequent addition of 10 mM *trans* Ca^{2+} (○).

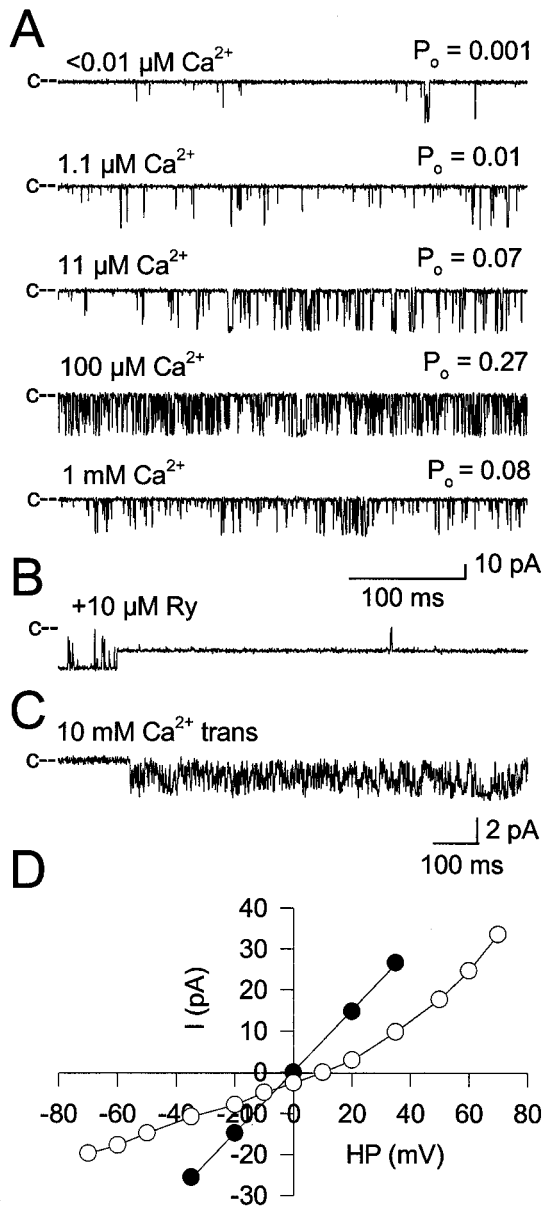

FIGURE 8 Single-channel recordings for mutant D4903A. Single-channel currents were recorded at −35 mV in symmetrical 250 mM KCl and are shown as downward inflections from a closed state (*c*–). (*A*) Effect of varied Ca^{2+} in the *cis* (cytosolic) chamber. (*B*) Single-channel recordings with 4 μM symmetrical Ca^{2+}; the addition of 10 μM ryanodine locks the channel in a ~50% conductance state. (*C*) Single-channel currents recorded at 0 mV in 250 mM KCl with 10 mM *trans* Ca^{2+} and 4 μM *cis* Ca^{2+}. (*D*) Current-voltage relationship of the expressed channel in 250 mM symmetrical KCl (●) and with the subsequent addition of 10 mM *trans* Ca^{2+} (○).

B in Figs. 8–10 shows the results of adding 10 μM ryanodine to activated channels. Ryanodine locked both D4903A (Fig. 8) and D4899N (Fig. 10) in a 50% conductance state, while G4894A (Fig. 9) was locked into a ~85% conductance state by *cis* ryanodine.

The ability of the mutants to conduct Ca^{2+} was determined by measuring single-channel currents at zero mV in symmetrical 250 mM KCl solutions containing 10 mM *trans* (SR lumenal) Ca^{2+} as the current carrier. Fig. 11 *A* shows traces of single-channel currents measured at 0 mV in 4 μM *cis* and either 4 μM (*top*) or 10 mM (*bottom*) *trans* Ca^{2+} for wt-RyR1 and mutant I4897L. An increase in *trans* Ca^{2+} resulted in a clearly discernible Ca^{2+} current of

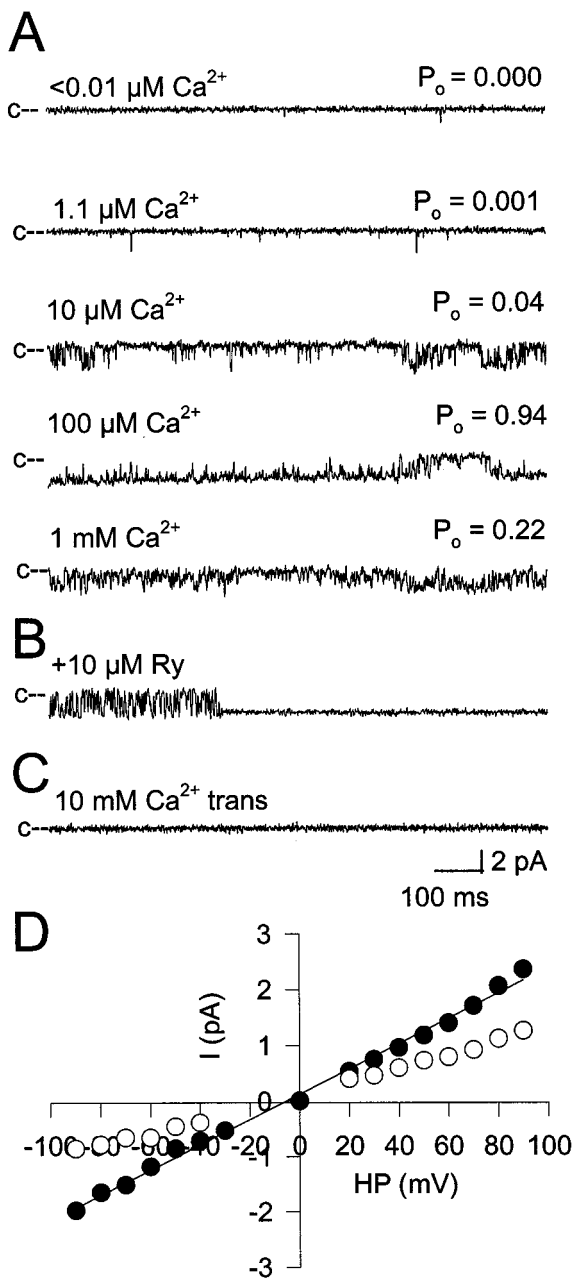

FIGURE 9 Single-channel recordings for mutant G4894A. Single-channel currents were recorded at −90 mV in symmetrical 250 mM KCl and are shown as downward inflections from a closed state (*c*–). (*A*) The effect of varied Ca^{2+} in the *cis* (cytosolic) chamber. (*B*) Single-channel recordings with 4 μM symmetrical Ca^{2+}; the addition of 10 μM ryanodine locks the channel in a ~85% conductance state. (*C*) Single-channel currents recorded at 0 mV in 250 mM KCl with 10 mM *trans* Ca^{2+} and 4 μM *cis* Ca^{2+}. (*D*) Current-voltage relationship of the expressed channel in 250 mM symmetrical KCl (●) and with the subsequent addition of 10 mM *trans* Ca^{2+} (○).

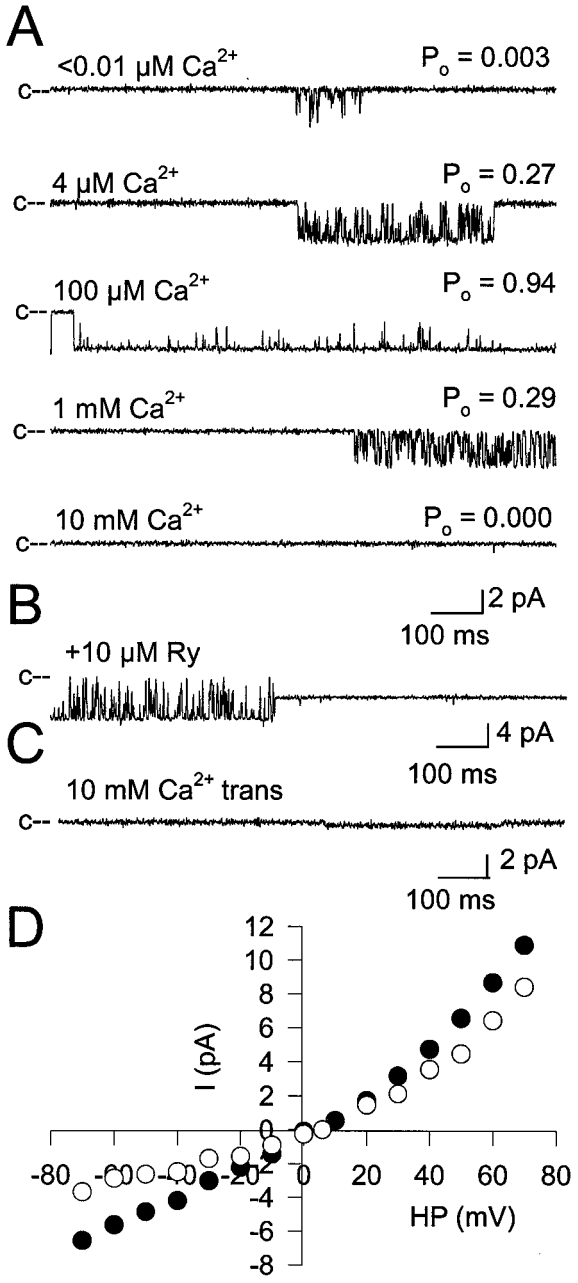

FIGURE 10 Single-channel recordings for mutant D4899N. Single-channel currents were recorded at −50 mV in symmetrical 250 mM KCl and are shown as downward inflections from a closed state (*c*–). (*A*) Effect of varied Ca^{2+} in the *cis* (cytosolic) chamber. (*B*) Single-channel recordings with 4 μM symmetrical Ca^{2+}; the addition of 10 μM ryanodine locks the channel in a ~50% conductance state. (*C*) Single-channel currents recorded at 0 mV in 250 mM KCl with 10 mM *trans* Ca^{2+} and 4 μM *cis* Ca^{2+}. (*D*) Current-voltage relationship of the expressed channel in 250 mM symmetrical KCl (●) and with the subsequent addition of 10 mM *trans* Ca^{2+} (○).

−2.7 ± 0.3 pA for wt-RyR1 (Table 1). I4897L showed a greatly reduced Ca^{2+} current of −0.5 ± 0.1 pA after the addition of 10 mM *trans* Ca^{2+}. D4903A (Fig. 8, *C* and *D*) and D4907A showed a calcium current similar to that of wild type (−2.4 ± 0.1 pA for D4903A and −2.4 ± 0.2 pA for D4907A; Table 1). G4894A did not show a measurable

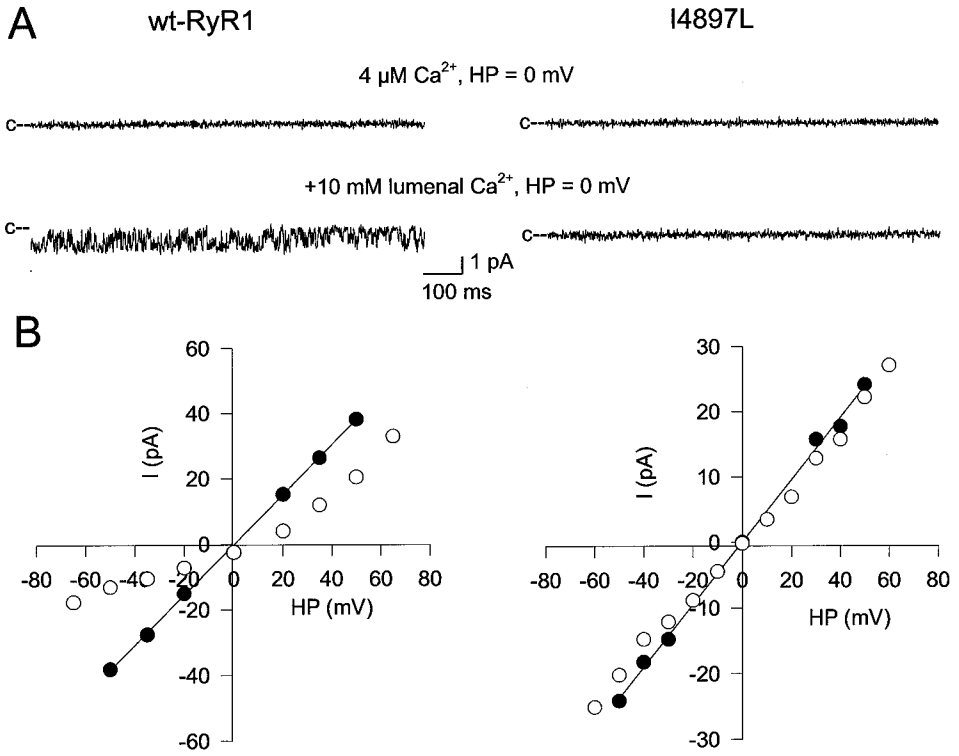

FIGURE 11 Single-channel recordings for wt-RyR1 and I4897L with K^+ and Ca^{2+} as charge carriers. (*A*) Single-channel currents were measured in symmetrical 250 mM KCl and 4 μM Ca^{2+} in 20 mM KHEPES (pH 7.4) at 0 mV (*top trace*) for wt-RyR1 (*left*) and I4897L (*right*) and after the addition of 10 mM *trans* Ca^{2+} (*bottom trace*). (*B*) *I-V* relationships for wt-RyR1 (*left*) and I4897L (*right*) before (●) and after (○) the addition of 10 mM *trans* Ca^{2+}.

Ca^{2+} current under these conditions, presumably because of very low conductance (Fig. 9 *C*). D4899N, another mutant channel with a low K^+ conductance, showed a greatly reduced Ca^{2+} current of -0.4 ± 0.1 pA at 0 mV (Fig. 10 *C* and Table 1). Mutations of I4899 (A, L, and V), D4899 (A and R), R4913E, and D4917A all showed greatly reduced Ca^{2+} currents after the addition of 10 mM *trans* Ca^{2+} at 0 mV relative to wt-RyR1 (Table 1) and had *I-V* relationships similar to that shown for I4897L in Fig. 11 *B*.

The voltage dependence of wt-RyR1 and five representative mutations are compared in Fig. 11 *B* for wt-RyR1 and I4897L and in Figs. 7–10 (*panel D*) for R4913E, D4903A, G4894A, and D4899N, respectively. *I-V* curves were recorded under two conditions in the presence of 250 mM symmetrical KCl 1) with 4 μM symmetrical Ca^{2+} (*filled circles*) and 2) with 4 μM *cis* and 10 mM *trans* Ca^{2+} (*empty circles*). The potassium currents measured in symmetrical Ca^{2+} were linear and showed ohmic voltage dependence, similar to that of the wild-type RyR1, with the exception of D4899N (Fig. 10 *D*), which showed nonohmic voltage dependence at positive potentials; the conductance reported for the D4899N mutation in Table 1 was obtained, therefore, at negative potentials only. The addition of 10 mM *trans* Ca^{2+} reduced the current and induced a rightward shift of the reversal potential of ~10 mV for wt-RyR1 (Fig. 11 *B*), D4903 (Fig. 8 *D*), and D4899N (Fig. 10 *D*). The addition of 10 mM *trans* Ca^{2+} reduced the K^+ current of G4894A at negative and positive holding potentials. Because of the very low conductance, this mutant failed to induce a detectable rightward shift in reversal potential. R4913E (Fig. 7 *B*) or I4897L (Fig. 11 *B*) did not exhibit a significant shift in reversal potential or the magnitude of K^+ currents after the addition of 10 mM *trans* Ca^{2+}. Results similar to those for R4913E and I4897L were observed for the remaining mutations I4897A and V, D4899A or R, and D4917A.

DISCUSSION

The results of this study suggest that the putative lumenal loop linking transmembrane domains M3 and M4 of RyR plays a crucial role in determining at least three of the most characteristic properties of the ryanodine receptor: Ca^{2+} activation, ryanodine binding, and ion conductance. Moreover, our results indicate that these three functions are not explicitly linked. One model (Balshaw et al., 1999) that can explain all of these results is illustrated in Fig. 12. The model suggests that a portion of the lumenal loop linking M3 to M4 in the RyR reenters the membrane, forming a P-segment analogous to those observed for many voltage-gated ion channels. The mutations did not appear to interfere with RyR tetramer formation, as all showed a sedimentation behavior comparable to that of wt-RyR1 during purification.

The most direct test of the model of Fig. 12 involved residue I4897, where three conservative mutations to A, L, and V yield channels with an altered ion conductance. The

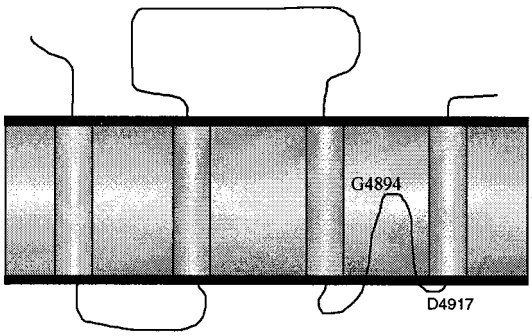

FIGURE 12 Proposed C-terminal arrangement for RyR, showing four transmembrane segments and a lumenal loop between M3 and M4. G4894 and D4917 indicate, respectively, the most N-terminal and C-terminal amino acids mutated in this study.

crystal structure of the *S. lividans* K^+ channel indicates that, within the pore-forming loop, there is an ion selectivity filter formed by a conserved GYG motif (Doyle et al., 1998). This motif is mimicked in the less ion selective RyRs with the sequence GIG and in the IP_3Rs, in which the I is replaced by a V. Mutations of I in the GIG motif and flanking residues would therefore be expected to alter the channel conductance, as is the case. The mutant conductances do not correspond to one-half of that of wild type and, therefore, likely do not represent a subconductance often observed for native channels. Mutation of Ile^{4987} yields channels that lack Ca^{2+} dependence, fail to bind ryanodine, and have atypical Ca^{2+} release in response to caffeine in a cell-based assay, in addition to altered ion conductance. One possibility we cannot rule out, therefore, is that global conformational changes account for the altered ion conductance and function of the I4897 mutants.

Mutations of amino acid residues that are identical in all types of RyRs and IP_3Rs sequenced to date show significant alterations in channel activity as compared to wt-RyR1. A conserved residue flanking the GIG motif of the RyRs is D4899. Replacement of the negatively charged aspartate with a hydrophobic alanine or positively charged arginine results in channels that are capable of releasing Ca^{2+} in response to caffeine in a cell-based assay, but which display an altered K^+ conductance and fail to bind ryanodine, suggesting that these three properties may not be implicitly linked. Alternatively, the mutant channels could be maintained in a "native" conformation in cells but undergo conformational changes during isolation that result in an altered K^+ conductance and pharmacology. A third mutation at this position to Asp, maintaining a polar side chain while losing the negative charge, yields a channel with properties very similar to those of the wild-type channel but with decreased conductances and an atypical gating behavior. G4894, also flanking the GIG motif, has recently been reported to affect the K^+ conductance of RyR2 while maintaining pharmacological regulation by Ca^{2+}, caffeine, and ryanodine (Zhao et al., 1999). Mutation of this residue to Ala in RyR1 also results in a channel, which maintains pharmacological regulation but shows a greatly decreased K^+ conductance (Fig. 9). G4894A in RyR1 fails to show a detectable Ca^{2+} current at 0 mV, although the K^+ conductance is reduced after the addition of an asymmetrical Ca^{2+} gradient, suggesting that the lack of current and relatively low percentage of cells responding to caffeine may be due to a very low Ca^{2+} conductance rather than a total lack of permeation by Ca^{2+} ions.

The recent report by Lynch et al. (1999) of a mutation resulting in malignant hyperthermia and central core disease also suggests that the lumenal domain of the ryanodine receptor plays a role in determining the Ca^{2+} sensitivity of the skeletal muscle RyR. It was found that a Mexican pedigree possesses a single mutation of I4898T (same residue as I4897 in rabbit RyR1), which sensitizes the RyR to Ca^{2+} activation, resulting in a channel that is partially activated at physiological cytosolic Ca^{2+} concentrations and is, therefore, "leaky." Our results, in contrast, suggest that the Thr mutation at this position is unique, as mutations to Ala, Val, and Leu all eliminate or greatly decrease the sensitivity to activating Ca^{2+}.

Mutation of a conserved Arg at position 4913 to a Glu resulted in a channel that was capable of releasing Ca^{2+} in response to caffeine in intact cells, but which failed to bind ryanodine. This mutation displayed greatly reduced K^+ and Ca^{2+} conductances, despite the replacement of a positively charged residue with a negatively charged residue. One explanation for this is that the change in charge destabilized the channel structure, thereby effecting global conformational changes during receptor isolation that are associated with receptor conductance and regulation.

Mutation of the absolutely conserved Asp at position 4917 to Ala resulted in a channel with a greatly decreased Ca^{2+} current, a lack of ryanodine binding, as well as caffeine-induced Ca^{2+} release. This residue is the final predicted amino acid of the lumenal loop before the beginning of the M4 transmembrane domain loop (Takeshima et al., 1989) and may play a role in directing the Ca^{2+} into the conduction pathway. Alternatively, the loss of the hydrophilic character at this position may result in global conformational changes that are associated with a loss of receptor regulation in intact cells.

In contrast to the mutations of conserved residues, two mutants involving amino acid residues not highly conserved among the RyR and IP_3R families show no significant changes in channel conductance and function. Mutation of D4903 (to A), which not is conserved in *C. elegans* (Ser) or lobster (Ala) RyRs and is a basic amino acid in most IP_3 receptor subtypes, had no apparent effect on RyR activity. Similarly, mutation of D4907 (to A), which is well conserved as either an Asp or Glu in all RyR or IP_3R subtypes except in *Pan Argus* IP_3R, in which it is a Lys, was without apparent effect on RyR activity.

Our mutations can therefore be grouped into four categories. The first of these are the two mutations (D4903A and D4907A) with no apparent defect, maintaining full single-channel conductance, as well as caffeine-induced calcium release, ryanodine binding, and single-channel pharmacology. The second category contains two residues (G4894A and D4899N) likely to be specifically reducing channel conductance, as indicated by the maintenance of pharmacological regulation. The third category includes those that appear to be functional ryanodine receptors, as evinced by caffeine-induced caffeine release, but which have an altered single-channel conductance and fail to show pharmacological regulation in vitro (D4899A and D4899R and R4913E). These channels may be structurally unstable outside of the intact cellular environment or require some cofactor, which is present in the cells but is lost upon isolation, to stabilize them in a pharmacologically active state. The final category contains mutations (I4897 A, L, and V, and D4917A) that have altered pharmacological regulation in both cellular and in vitro assays but maintain a low potassium conductance. These mutations are likely to have a major impact on the structure of the channel or on the conformational changes linking ligand binding to functional response. The mutations at I4897 may only weakly interact with a hydrophobic cleft normally occupied by the branched side chain of the Ile residue, placing the backbone carbonyls into the pore, where they contribute to the ion conduction pathway. D4917, being the final residue at the lumenal end of transmembrane domain 4, may be directly involved in stabilizing the transmembrane arrangement of the channel.

The use of confocal microscopy for analysis of caffeine-induced Ca^{2+} release, while providing a means of identifying individual cells responding to the drug, has several limitations. Foremost among these is that the images are limited to a plane through the cells of ~ 1 μm; therefore cells that are not in that focal plane will have a lower fluorescence, and the fluorescence intensity may respond differently to the drug. This technique also has a limited temporal resolution, making kinetic analysis of the caffeine release difficult to interpret. Nonetheless, it is our opinion that the technique does allow for a qualitative determination of caffeine-induced Ca^{2+} release. This is supported by the fact that several of our mutations (G4894A, D4899, D4903A, D4907A) maintain apparently normal caffeine-induced Ca^{2+} release and Ca^{2+} dependence of [^{3}H]ryanodine binding and single-channel activities, while others, with significant apparent defects in in vitro assays, display an altered Ca^{2+} release. As pointed out above, the apparent disagreement between the results of cellular Ca^{2+} release and those of in vitro pharmacology may be due to a decrease in the stability of the expressed channel proteins and hence to a disparity between data for experiments performed in intact cells and with isolated channels.

The Ca^{2+} activation (Chen et al., 1993, 1998; Bhat et al., 1997b) and Ca^{2+} inactivation sites (Nakai et al., 1999; Du and MacLennan, 1998), as well as the high-affinity [^{3}H]ryanodine binding site (Callaway et al., 1994; Witcher et al., 1994), have been localized to the C-terminal one-fourth of RyR1. However, protein conformational changes mediated by the N-terminal portion have been shown to affect RyR1 function. Unlike the full-length RyR1, a truncated RyR1 (Δ1–3660) failed to close at high [Ca^{2+}], suggesting that the N-terminal foot structure has a role in Ca^{2+} regulation (Bhat et al., 1997b). Consistent with this finding, single amino acid mutations in the N-terminal and central regions of RyR1 link to a rare muscle disorder known as malignant hyperthermia, which is characterized by elevated Ca^{2+} release from SR (Phillips et al., 1996). In support of a long-range control of [^{3}H]ryanodine binding is that replacement of RyR1 regions with corresponding RyR2 regions not involving the C-terminal one-fourth of the receptor results in the loss or reduction of [^{3}H]ryanodine binding (Nakai et al., 1999). Therefore, it is likely that interactions between both the N- and C-terminal portions of the ryanodine receptor are crucial for all aspects of channel Ca^{2+} dependence. The present study suggests that the M3-M4 lumenal loop affects these interactions, directly or indirectly, as amino acid substitutions in this region cause the loss of Ca^{2+} activation and high-affinity ryanodine binding, in addition to an altered ion conductance.

In conclusion, our results suggest that single amino acid residue changes in the lumenal M3-M4 loop affect local events (channel conductance) as well as more global events (Ca^{2+} dependence and ryanodine binding). The data that are most consistent with our hypothesis that the M3-M4 lumenal loop contributes to the structure of the pore come from the changes we observe in ion conductance. The fact that mutation of several conserved residues in close proximity to each other has such profound effects on ion conductance, while mutations of less conserved residues in the same region result in no detectable defect, lends credence to our conclusion. Nonetheless, further studies are necessary that are beyond the scope of this work. These include the possibility of scanning cysteine mutagenesis, as has been applied to examination of the pore structure of voltage-gated and ligand-gated ion channels (Dart et al., 1998; Yamagishi et al., 1997), as well as a more detailed investigation of channel permeation, selectivity, and gating.

We thank Dr. John Lemasters and the Cell and Molecular Imaging Facility at the University of North Carolina at Chapel Hill for the use of the BioRad MRC-600. The help of Daniel Pasek in purifying the ryanodine receptors is gratefully acknowledged.

This work was supported by National Institutes of Health grant AR18687.

REFERENCES

Balshaw, D., L. Gao, and G. Meissner. 1999. Luminal loop of the ryanodine receptor: a pore-forming segment? *Proc. Natl. Acad. Sci. USA.* 96:3345–3347.

Bhat, M. B., J. Y. Zhao, S. Hayek, E. C. Freeman, H. Takeshima, and J. J. Ma. 1997a. Deletion of amino acids 1641–2437 from the foot region of skeletal muscle ryanodine receptor alters the conduction properties of the Ca release channel. *Biophys. J.* 73:1320–1328.

Bhat, M. B., J. Y. Zhao, H. Takeshima, and J. J. Ma. 1997b. Functional calcium release channel formed by the carboxyl-terminal portion of ryanodine receptor. *Biophys. J.* 73:1329–1336.

Callaway, C., A. Seryshev, J. P. Wang, K. J. Slavik, D. H. Needleman, C. I. Cantu, Y. Wu, T. Jayaraman, A. R. Marks, and S. L. Hamilton. 1994. Localization of the high and low affinity [^{3}H]ryanodine binding sites on the skeletal muscle Ca^{2+} release channel. *J. Biol. Chem.* 269: 15876–15884.

Chen, S. R., K. Ebisawa, X. Li, and L. Zhang. 1998. Molecular identification of the ryanodine receptor Ca^{2+} sensor. *J. Biol. Chem.* 273: 14675–14678.

Chen, S. R. W., L. Zhang, and D. H. MacLennan. 1993. Antibodies as probes for Ca^{2+} activation sites in the Ca^{2+} release channel (ryanodine receptor) of rabbit skeletal muscle sarcoplasmic reticulum. *J. Biol. Chem.* 268:13414–13421.

Coronado, R., J. Morrissette, M. Sukhareva, and D. M. Vaughan. 1994. Structure and function of ryanodine receptors. *Am. J. Physiol.* 266: C1485–C1504.

Dart, C., M. L. Leyland, P. J. Spencer, P. R. Stanfield, and M. J. Sutcliffe. 1998. The selectivity filter of a potassium channel, murine kir2.1, investigated using scanning cysteine mutagenesis. *J. Physiol. (Lond.).* 511:25–32.

Doyle, D. A., J. Morais Cabral, R. A. Pfuetzner, A. Kuo, J. M. Gulbis, S. L. Cohen, B. T. Chait, and R. MacKinnon. 1998. The structure of the potassium channel: molecular basis of K^+ conduction and selectivity. *Science.* 280:69–77.

Du, G. G., and D. H. MacLennan. 1998. Functional consequences of mutations of conserved, polar amino acids in transmembrane sequences of the Ca^{2+} release channel (ryanodine receptor) of rabbit skeletal muscle sarcoplasmic reticulum. *J. Biol. Chem.* 273:31867–31872.

Franzini-Armstrong, C., and F. Protasi. 1997. Ryanodine receptors of striated muscles: a complex channel capable of multiple interactions. *Physiol. Rev.* 77:699–729.

Gao, L., A. Tripathy, X. Lu, and G. Meissner. 1997. Evidence for a role of C-terminal amino acid residues in skeletal muscle Ca^{2+} release channel (ryanodine receptor) function. *FEBS Lett.* 412:223–226.

Gao, L., A. Tripathy, L. Xu, D. Pasek, D. Balshaw, L. Xin, G. Meissner. 1999. Mutation of charged amino acids in a putative lumenal loop of the skeletal muscle Ca^{2+} release channel results in the loss of high affinity [^{3}H]ryanodine binding. *Biophys. J.* 76:A303.

Grunwald, R. 1996. Membrane topology and proteolytic fragmentation pattern of the skeletal muscle ryanodine receptor. Ph.D. thesis. University of North Carolina at Chapel Hill.

Grunwald, R., and G. Meissner. 1995:Lumenal sites and C terminus accessibility of the skeletal muscle calcium release channel (ryanodine receptor). *J. Biol. Chem.*270:11338–11347.

Lee, H. B., L. Xu, and G. Meissner. 1994. Reconstitution of the skeletal muscle ryanodine receptor-Ca^{2+} release channel protein complex into proteoliposomes. *J. Biol. Chem.* 269:13305–13312.

Lynch, P. J., J. F. Tong, M. Lehane, A. Mallet, L. Giblin, J. A. Heffron, P. Vaughan, G. Zafra, D. H. MacLennan, and T. V. McCarthy. 1999. A mutation in the transmembrane/luminal domain of the ryanodine receptor is associated with abnormal Ca^{2+} release channel function and severe central core disease. *Proc. Natl. Acad. Sci. USA.* 96:4164–4169.

Marty, I., M. Villaz, G. Arlaud, I. Bally, and M. Ronjat. 1994. Transmembrane orientation of the N-terminal and C-terminal ends of the ryanodine receptor in the sarcoplasmic reticulum of rabbit skeletal muscle. *Biochem. J.* 298:743–749.

Meissner, G. 1994. Ryanodine receptor/Ca^{2+} release channels and their regulation by endogenous effectors. *Annu. Rev. Physiol.* 56:485–508.

Nakai, J., L. Gao, L. Xu, C. Xin, D. A. Pasek, and G. Meissner. 1999. Evidence for a role of C-terminus in Ca^{2+} inactivation of skeletal muscle Ca^{2+} release channel (ryanodine receptor). *FEBS Lett.* 459:154–158.

Phillips, M. S., J. Fujii, V. K. Khanna, S. DeLeon, K. Yokobata, P. J. de Jong, and D. H. MacLennan. 1996. The structural organization of the human skeletal muscle ryanodine receptor (RYR1) gene. *Genomics.* 34:24–41.

Rousseau, E., J. Ladine, Q. Y. Liu, and G. Meissner. 1988. Activation of the Ca^{2+} release channel of skeletal muscle sarcoplasmic reticulum by caffeine and related compounds. *Arch. Biochem. Biophys.* 267:75–86.

Serysheva, I. I., E. V. Orlova, W. Chiu, M. B. Sherman, S. L. Hamilton, and M. van Heel. 1995. Electron cryomicroscopy and angular reconstruction used to visualize the skeletal muscle calcium release channel. *Nature Struct. Biol.* 2:18–23.

Sutko, J. L., and J. A. Airey. 1996. Ryanodine receptor Ca^{2+} release channels: does diversity in form equal diversity in function? *Physiol. Rev.* 76:1027–1071.

Takeshima, H., S. Nishimura, T. Matsumoto, H. Ishida, K. Kangawa, N. Minamino, H. Matsuo, M. Ueda, M. Hanaoka, T. Hirose, and S. Numa. 1989. Primary structure and expression from complementary DNA of skeletal muscle ryanodine receptor. *Nature.* 339:439–445.

Tripathy, A., L. Xu, G. Mann, and G. Meissner. 1995. Calmodulin activation and inhibition of skeletal muscle Ca^{2+} release channel (ryanodine receptor). *Biophys. J.* 69:106–119.

Wagenknecht, T., R. Grassucci, J. Berkowitz, G. J. Wiederrecht, H. B. Xin, and S. Fleischer. 1996. Cryoelectron microscopy resolves FK506-binding protein sites on the skeletal muscle ryanodine receptor. *Biophys. J.* 70:1709–1715.

Witcher, D. R., P. S. McPherson, S. D. Kahl, T. Lewis, P. Bentley, M. J. Mullinnix, J. D. Windass, and K. P. Campbell. 1994. Photoaffinity labeling of the ryanodine receptor/Ca^{2+} release channel with an azido derivative of ryanodine. *J. Biol. Chem.* 269:13076–13079.

Yamagishi, T., M. Janecki, E. Marban, and G. F. Tomaselli. 1997. Topology of the P segments in the sodium channel pore revealed by cysteine mutagenesis. *Biophys. J.* 73:195–204.

Zhao, M., P. Li, X. Li, L. Zhang, R. J. Winkfein, and S. R. Chen. 1999. Molecular identification of the ryanodine receptor pore-forming segment. *J. Biol. Chem.* 274:25971–25974.

Zorzato, F., J. Fujii, K. Otsu, M. Phillips, N. M. Green, F. A. Lai, G. Meissner, and D. H. MacLennan. 1990. Molecular cloning of cDNA encoding human and rabbit forms of the Ca^{2+} release channel (ryanodine receptor) of skeletal muscle sarcoplasmic reticulum. *J. Biol. Chem.* 265:2244–2256.